McArthur, A.D., and Tek, D.E., 2021, Controls on the origin and evolution of deep-ocean trench-axial channels: Geology, v. 49,
https://doi.org/10.1130/G48612.1

Supplementary material 1. Acquisition, processing and interpretation of seismic data.

2D dataset

The PEG14 2D seismic reflection dataset was collected by WesternGeco in 2014 and reprocessed in 2016. This survey constitutes 5242 line-km across the Hikurangi Margin (Fig. S1), covering some 350 km along the trench. Data were collected in a frequency range of 3–200 Hz and full stack data are depth converted. In this dataset, a downward decrease in acoustic impedance is represented by a trough (white), and a downward increase is represented by a peak (black). Data were interpreted using the Petrel E&P software platform. Major faults and structures were interpreted and regional surfaces were extrapolated from the survey, using information obtained from from Ghisetti et al., (2016); McArthur et al., (2019); and Barnes et al., (2020).

3D dataset

This study employed 2600 km2 of pre-stack Kirchoff depth migrated 3D seismic data, acquired at broadband frequency in 2017 by WesternGeco. This dataset images a ca 150 km long stretch of the Hikurangi Trench and Channel (Fig. S1). Full stack data are displayed SEG positive; a downward decrease in acoustic impedance is shown as a trough (white reflection). Data were interpreted using Petrel E&P software. Major faults and channel fills were interpreted. Variance attribute analysis was used to highlight channel forms on interpreted surfaces.

References

Barnes, P.M., Wallace, L.M., Saffer, D.M., Bell, R.E., Underwood, M.B., Fagereng, A., Meneghini, F., Savage, H.M., Rabinowitz, H.S., Morgan, J.K., and Kitajima, H., 2020, Slow slip source characterized by lithological and geometric heterogeneity: Science Advances, v. 6, p.eaay3314.

Ghisetti, F.C., Barnes, P.M., Ellis, S., Plaza-Faverola, A.A. and Barker, D.H., 2016, The last 2 Myr of accretionary wedge construction in the central Hikurangi margin (North Island, New Zealand): Insights from structural modeling: Geochemistry, Geophysics, Geosystems, v. 17, p.2661-2686.

McArthur, A.D., Claussmann, B., Bailleul, J., McCaffrey, W., and Clare, A., 2019, Variation in syn-subduction sedimentation patterns from inner to outer portions of deep-water fold and thrust belts: examples from the Hikurangi subduction margin of New Zealand: Geological Society, London, Special Publications, v. 490, p. 285-310.

Figure S1. Location of seismic datasets courtesy of WesternGeco.

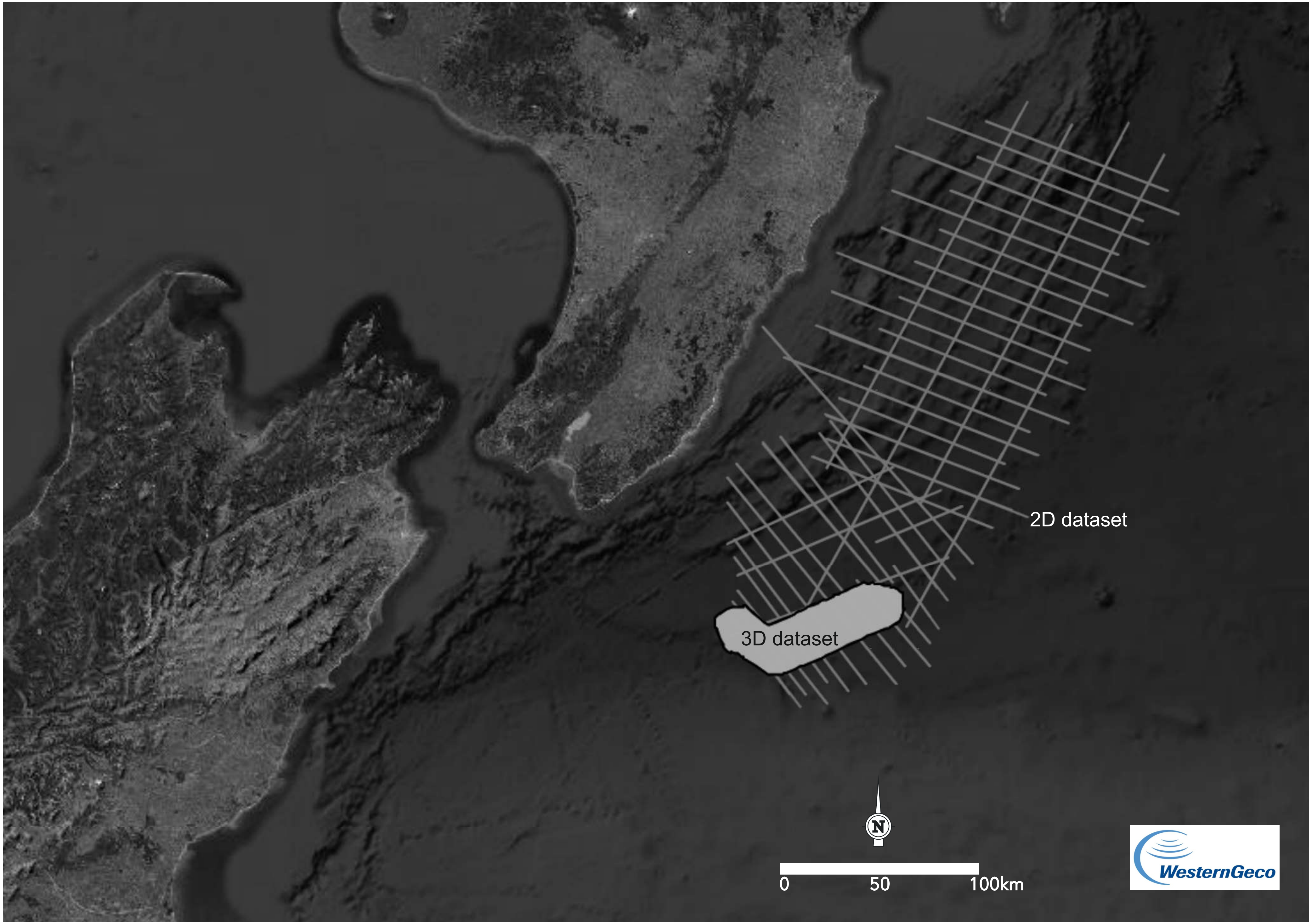

Figure S2. Non interpreted seismic line in the southern, proximal part of the Hikurangi Trench.

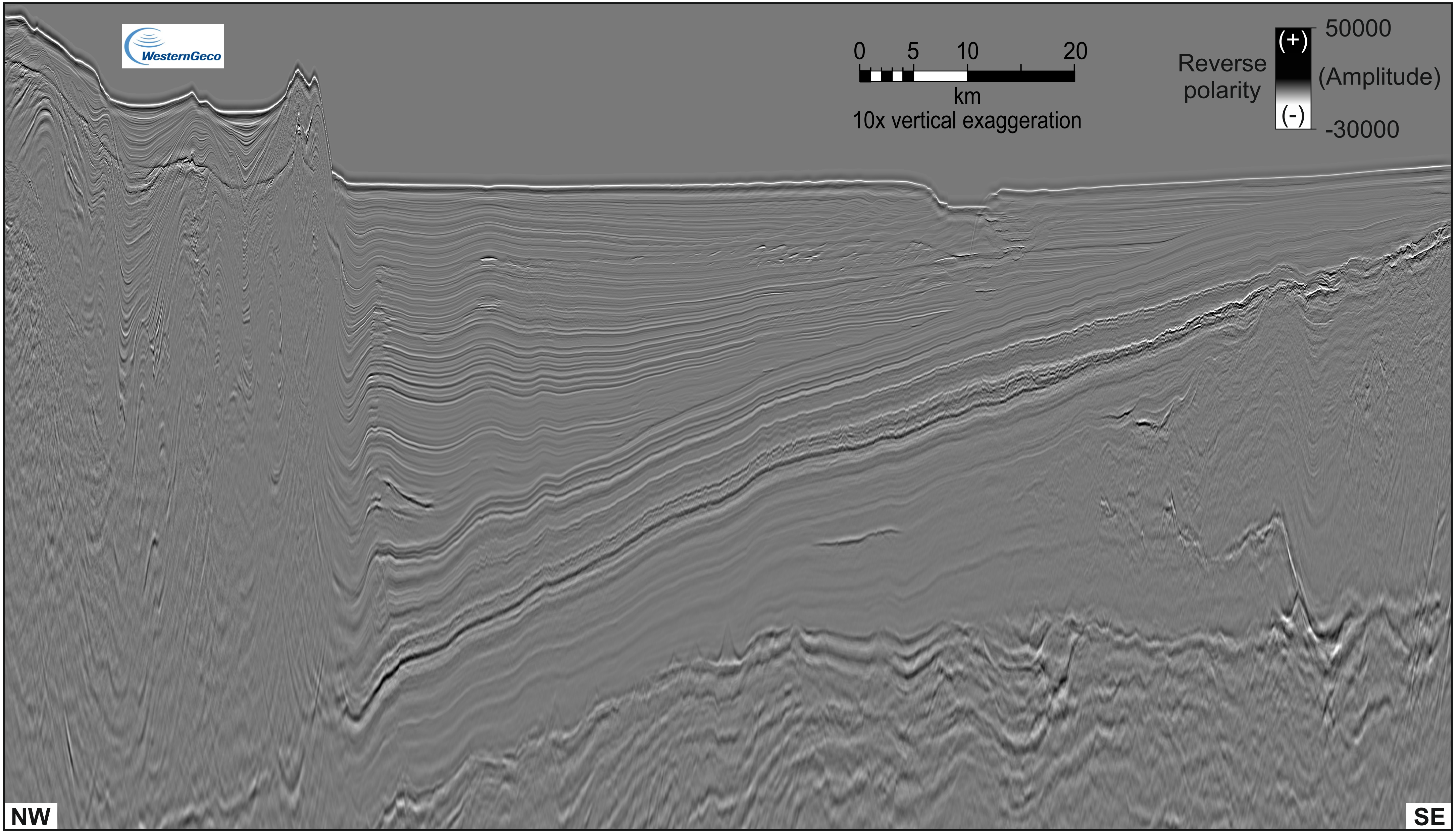

Figure S3. Non interpreted seismic line in the northern, distal part of the Hikurangi Trench.

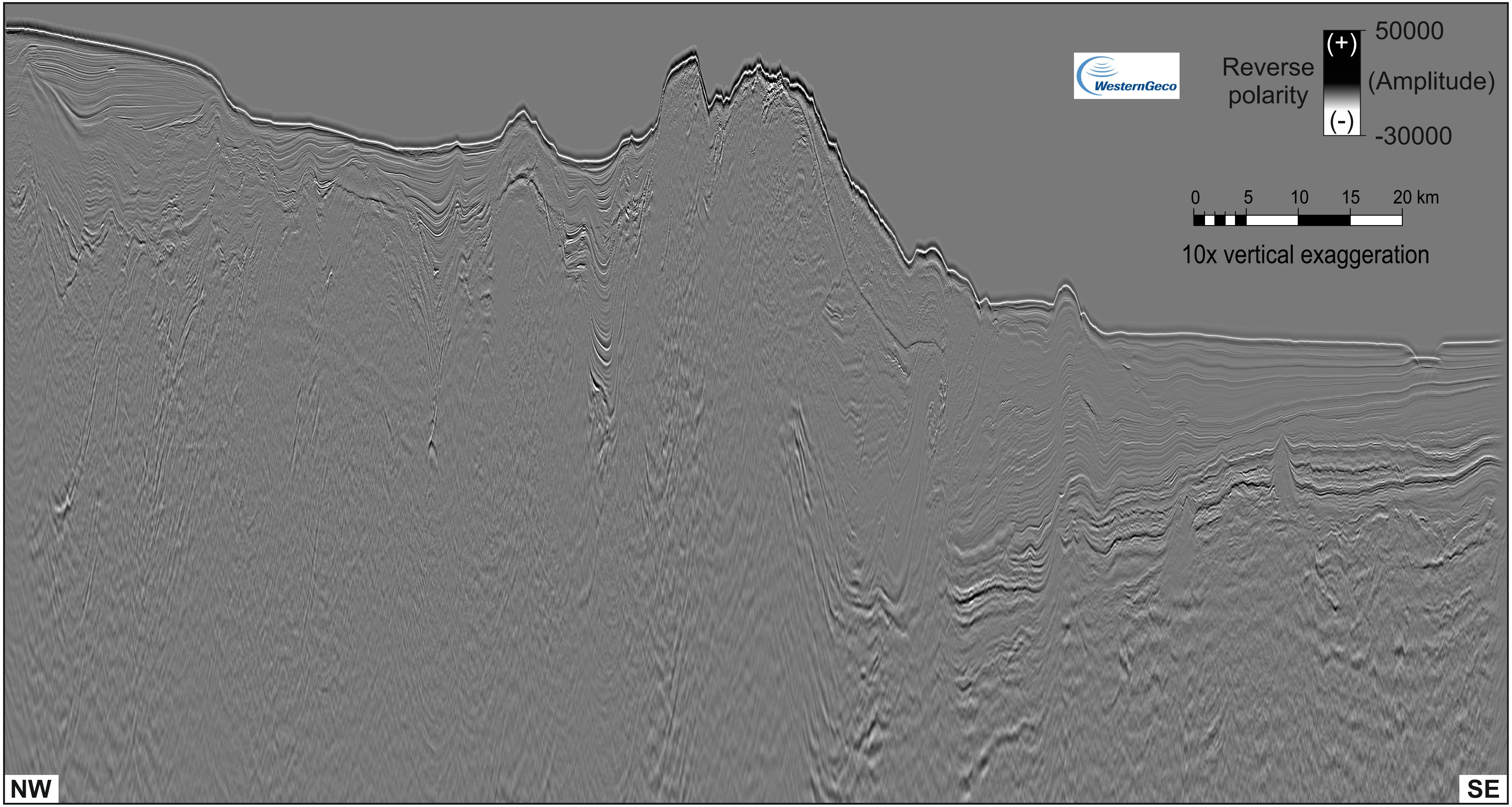

Table S1. Dimensional and morphometric measurements from global subduction trenches.

Trench name	Lattituide	Type	Trench length	Trench width	Trench depth	Trench gradient	Rugosity	Trench age	Sedimentary cover	Filled	Sediment type	Av. sediment supply	Convergence rate	Climate	Catchment gradient	Axial channel (y/n)	Type (today)	Channel length km	Length in trench km	Gradient slope vs trench	Channel axis gradient	Single / multi source	Channel age Ma	References
Hikurangi Trench	38 - 42o S	Mixed siliciclastic / volcaniclastic	720 km	12-70 km	3-3.75 km	0.5o to NE	Low	~27 Ma	1-6 km	Filled	Coarse siliciclastics	High (7200 ± 1500 T/km2 yr)	38-50 mm/yr	Temperate	Moderate	Hikurangi Channel	Aggradational	2000	605	8o	0.05o	6	3.5	Lewis 1994; Mountjoy et al., 2018
Kermadec Trench	25 - 37o S	Volcanic	1565 km	~50 km	7-10 km	1-4o NNE	Moderate	~25 Ma	~200 -500 m	Under	Fine with volcanics	High (170 x10*12 g/yr)	80-85 mm /yr	Equatorial	Low (submarine)	N	NA	NA		NA	NA	NA	NA	Ballance et al., 1999
Tonga Trench	14-24o S	Volcanic	1300 km	15-30 km	10.8 km	3o E to SW	Moderate	~44 Ma	~200 m	Under	Fine with volcanics	High (170 x10*12 g/yr)	60-240 mm/yr	Equatorial	Low (mostly submarine)	N	NA	NA		NA	NA	NA	NA	Ballance et al., 1989; Clift et al., 1998
New Hebrides	10-23o S	Volcanic	1200 km	70 km	9 km	3o to W	Moderate	55-42 Ma	~300 m	Under	Fine with volcanics	High (180 x10*12 g/yr)	100-130 mm/yr	Equatorial	Low (mostly submarine)	N	NA	NA		NA	NA	NA	NA	Fisher et al., 1991
San Cristobal	8-10o S	Volcanic	600 km	11 km	8.2 km	3o to E	Low	~10-5 Ma	Minimal	Under	Fine with volcanics	High (180 x10*12 g/yr)	100 mm/yr	Equatorial	Low (mostly submarine)	N	NA	NA		NA	NA	NA	NA	Tregoning et al., 1998a; Mann and Taira 2004
North Solomon	6-10o S	Volcanic	900 km	10-20 km	4.3 km	2o to SE	Moderate	5 Ma	0-1 km	Under	Fine with volcanics	High (180 x10*12 g/yr)	100 mm/yr	Equatorial	Moderate	N	NA	NA		NA	NA	NA	NA	Phinney et al., 2004; Tairaa et al., 2004
Bougainville Trench	6-7o S	Mixed siliciclastic / volcaniclastic	840 km	50-75 km	9.1 km	4o to E	Low	~5 Ma	0-3 km	Under	Coarse siliciclastics,	High (180 x10*12 g/yr)	80-150 mm/yr	Equatorial	Moderate	Markham Canyon	Erosional	235	55	14o	2.6o	6	5	Davies et al., 1986; Tiffin et al., 1987; Tregoning et al., 1998b
Melanesian Trench	0-5o S	Volcanic	1680 km	20-40 km	6.7 km	2.5o	Low	45 Ma	up to 1500 m	Under	Carbonates and volcaniclastics	High (180 x10*12 g/yr)	124 mm/yr	Equatorial	Low (mostly submarine)	N	NA	NA		NA	NA	NA	NA	Exon and Tiffin 1982; Holme et al 2016
New Guinea Trench	0-2o S	Mixed siliciclastic / volcaniclastic	700 km	30-40 km	5.2 km	1.3o W	Low	~9 Ma	up to 1 km	Under	Coarse siliciclastics,	High (180 x10*12 g/yr)	70 mm/yr	Equatorial	Moderate	N	NA	NA		NA	NA	NA	NA	Milsom et al., 1992; Tregoning and Gorbatov, 2004
Philippine Trench	2-15o N	Mixed volcaniclastic / siliciclastic	1320 km	10-15 km	10.5 km	3o to S	Moderate	8-9 Ma	0-1500 m	Under	Fine with volcanics	Low (70 x10*12 g/yr)	30 mm/yr	Equatorial	Low (mostly submarine)	N	NA	NA		NA	NA	NA	NA	Nichols et al., 1990; Lallemand et al., 1998
Sunda Trench	17o N to 12o S	Mixed **siliciclastic**/ volcaniclastic	5400 km	20-30 km	3-6.5 km	1.1o to SE	Low	~33 Ma	1.5 - 6 km	Under to overfilled	Coarse siliciclastics	Very high 50 g cm 2 kyr 1	47 mm/yr	Equatorial	High to low	Sunda Channel	Aggradational	875	875	6.6o	1o	2	10	Moore et al., 1982a; Mosher et al., 2004; Pickering et al., 2020
Manila Trench	12-20o N	Mixed **siliciclastic**/ volcaniclastic	990 km	5-60 km	5.4 km	1.8o to S	High	~30 Ma	<2.6 km	Filled	Coarse siliciclastics	High but variable	20-100 mm/yr	Equatorial	High to moderate	Mompong Canyon	Erosional	64	64	30o	3.4o	6	1	Hayes and Lewis, 1984; Lewis and Hayes, 1984
Northern end												6.6 Mton/yr				Gaoping Canyon	Erosional	450	175	19o	0.5o	1	1	Huh et al., 2009; Gavey et al., 2017
Mariana Trench	11-25o N	Volcanic	2550 km	50-75 km	10.9 km	3o (E & S)	High	~7 Ma	0-300 m	Under	Fine with volcanics	Low (70 x10+12 g/yr)	110-180 mm/yr	Equatorial	Low (mostly submarine)	N	NA	NA		NA	NA	NA	NA	Fryer, 1995
Izu-Ogasawara	26-34o N	Mixed volcaniclastic / siliciclastic	900 km	5-20 km	9.8 km	3o S	Moderate	~43 Ma	0-2 km	Under	Mostly volcanics,	Low (80 x10*12 g/yr)	98 mm/yr	Temperate	Low (mostly submarine)	N	NA	NA		NA	NA	NA	NA	Soh et al., 1988; Stern and Bloomer, 1992
Ryukyu Trench	23-34o N	Mixed volcaniclastic / siliciclastic	1400 km	10-25 km	7.5 km	2.5o	High	33 Ma	0-3 km	Filled	Mostly volcanics,	Low (70 x10*12 g/yr)	52 - 98 mm/yr	Temperate	Low (mostly submarine)	Shih-t'I Pi Canyon	Erosional	237	117	19o	2.3o	25	1	Nishizawa et al., 2017
Nankai Trough	31-34o N	Mixed **siliciclastic**/ volcaniclastic	750 km	15-30 km	5 km	1.2o SW	Low	~19 Ma	1 km	Filled	Coarse siliciclastics	Low (70 x10*12 g/yr)	43 mm/yr	Temperate	Moderate	Nankai Channel	Aggradational	430	335	20o	0.9o	4	0.5	Shimamura, 1989; Underwood et al., 2010
Japan Trench	34-40o N	Mixed volcaniclastic / siliciclastic	800 km	5-20 km	8 km	2o S	High	~20-25 Ma	0-1 km	Under	Fine siliciclastics	Low (50 x10*12 g/yr)	79-92 mm/yr	Temperate	Moderate	n	NA	NA		NA	NA	NA	NA	von Huene et al., 1982
Kuril-Kamchatka	41-55o N	Mixed volcaniclastic / siliciclastic	2500 km	1-15 km	10.5 km	1.7o	Moderate	~80 Ma	0-3 km	Under	Dominantly volcaniclastics	Low (50 x10*12 g/yr)	75-83 mm/yr	Sub-polar	Low (mostly submarine)	n	NA	NA		NA	NA	NA	NA	Scholl, 1974; Gnibidenko et al., 1983
Aleutian Trench	55-59o N	Mixed volcaniclastic / siliciclastic	3400 km	15-45 km	7.8 km	0.7o W	Moderate	30-35 Ma	1-2 km	Under	Dominantly volcaniclastics	Moderate (110 x10*12 g/yr)	75 mm/yr	Sub-polar	Low	n	NA	NA		NA	NA	NA	NA	Scholl, 1974; Delong et al., 1978; Underwood, 1986
Eastern Aleutian		Mixed **siliciclastic**/ volcaniclastic								Filled	Coarse siliciclastics	Moderate (110 x10*12 g/yr)	75 mm/yr	Sub-polar	Moderate	Surveyor Channel	Aggradational	700	300	4.3o	0.45o	8	5	Ness and Klum ,1973
Cascadia	40-50o N	Mixed **siliciclastic**/ volcaniclastic	1200 km	30-100 km	3.1 km	1.9o S	Low	42 Ma	1-7 km	Overfilled	Coarse siliciclastics	Moderate (100 x10*12 g/yr)	21-44 mm/yr	Temperate	High to moderate	Astoria Channel	Aggradational	550	550	20o	0.28o	8	1	Komar, 1973; Davis and Hyndman, 1989; Wolf and Hamer, 1999; Goldfinger et al., 2012
Middle America	8-21o N	Mixed **siliciclastic**/ volcaniclastic	2750 km	5-25 km	6.7 km	1.2o	High	~100 Ma	<1 km	Under	Coarse siliciclastics	Very Low (20 x10*12 g/yr)	70 - 100 mm/yr	Equatorial	Moderate	Ometepec Canyon	Aggradational	27	27	15o	0.5o	1	1	McMillen et al., 1982; Moore et al., 1982b; Watkins, 1989
Colombian Trench	6o N to 1o S	Mixed volcaniclastic / siliciclastic	730 km	10-50 km	4 km	2o S	High	~25 Ma	<1 km	Under	Fine with volcanics	Very Low (20 x10*12 g/yr)	50-64 mm/yr	Equatorial	Moderate	n	NA	NA		NA	NA	NA	NA	Mountney and Westbrook, 1997
Ecuador Trench	0o N to 3o S	Mixed volcaniclastic / siliciclastic	400 km	1-5 km	4.5 km	2.8o S	High	~26 Ma	<1 km	Under	Fine with volcanics	Very Low (10 x10*12 g/yr)	60 mm/yr	Equatorial	High	n	NA	NA		NA	NA	NA	NA	Lonsdale 1978; Collot et al., 2002
Peru Trench	3-14o S	Mixed volcaniclastic / siliciclastic	1200 km	10-20 km	6.5 km	1.6o	High	~23 Ma	200 - 500 m	Under	Fine with volcanics	Very Low (10 x10*12 g/yr)	61 mm/yr	Arid	High	n	NA	NA		NA	NA	NA	NA	Klum 1981; Krabbenhöft et al., 2004
Chile Trench	15- 57o S	Mixed **siliciclastic**/ volcaniclastic	5200 km	7 - 65 km	8 km	0.7o N	Moderate	~23 Ma	100 - 1000 m	Under to overfilled	Coarse siliciclastics	Very Low (10 x10*12 g/yr)	100-110 mm/yr	Arid	High	n	NA	NA		NA	NA	NA	NA	Schweller and Kulm, 1978; Thornberg et al., 1990
Southern Chile	32S									Filled	Coarse siliciclastics	Very Low (10 x10*12 g/yr)	100-110 mm/yr	Temperate	High	Axial Channel	Aggradational	1000	1000	12o	0.06o	14	1	Thornberg et al., 1990
South Sandwich	54-60o S	Volcaniclastics	1230 km	5-70 km	8.2 km	2.7o	High	~15 Ma	<500 m	Under	Fine with volcanics	Very Low (5 x10*12 g/yr)	67-81 mm/yr	Polar	Low (mostly submarine)	n	NA	NA		NA	NA	NA	NA	Larter et al., 2003
Hjort Trench	55-59o S	Volcaniclastics	490 km	2.5 - 10 km	6.6 km	3.2o S	Moderate	~20 Ma	500 - 1500 m	Under	Fine with volcanics	Very Low (5 x10*12 g/yr)	5-26 mm /yr	Polar	Low (all submarine)	n	NA	NA		NA	NA	NA	NA	Meckel et al., 2003
Puysegur Trench	46-49o S	Volcaniclastics	340 km	5-10 km	6.4 km	3.3o	Moderate	~10 Ma	<1 km	Under	Fine with volcanics	Very Low (5 x10*12 g/yr)	32-35 mm/yr	Temperate	Low (all submarine)	n	NA	NA		NA	NA	NA	NA	Collot et al., 1995; Melhuish et al., 1999
Puerto Rico Trench	15-18o N	Mixed volcaniclastic / siliciclastic	820 km	10-20 km	8.3 km	2.7o W	Moderate	~70 Ma	100-3000 m	Filled	Coarse siliciclastics,	Very Low (10 x10*12 g/yr)	17-23 mm/yr	Equatorial	Low	Vidal Channel	Aggradational	930	100	1o	0.09o	10	1	Larue and Ryan, 1998; Deville et al., 2015
Lesser Antilies	9-14o N	Mixed **siliciclastic**/ volcaniclastic	560 km	10-50 km	5.5 km	0.9o N	Low	80-105 Ma	400 - 3000 m	Overfilled	Coarse siliciclastics,	High 210 × 10*6 ton/a	11-14 mm/yr	Equatorial	Low	Orinoco Channel	Aggradational	6000	250	9o	0.7o	7	40	Westbrook et al., 1984; López et al., 2006; Callec et al., 2010; Deville et al., 2015
Calabrian Trench	35-37o N	Mixed **siliciclastic**/ volcaniclastic	300 km	5-10 km	4 km	0.5o	Low	~30 Ma	750 - 3500 m	Overfilled	Fine siliciclastics and salt	High (210 x10*12 g/yr)	4-5 mm/yr	Temperate	Low	n	NA	NA		NA	NA	NA	NA	Minelli and Faccenna, 2010; Polonia et al., 2011
Hellenic Trench	33-37o N	Mixed **siliciclastic**/ volcaniclastic	1150 km	2.5 - 10 km	5.3 km	2.8o	Low	45 Ma	500-1000 m	Overfilled	Fine siliciclastics and salt	High (210 x10*12 g/yr)	30-60 mm/yr	Temperate	Low	n	NA	NA		NA	NA	NA	NA	Stanley and Maldonado, 1981; Huchon et a., 1982; Brun and Sokoutis, 2010
Makran Trench	24o N	Siliciclastic	1000 km	5-50 km	3.5 km	1.2o W	Low	~65 Ma	1500 - 7500 m	Overfilled	Fine siliciclastics	High (210 x10*12 g/yr)	40 mm/yr	Arid	Moderate	Axial Channel	Erosional	185	24	23o	0.2o	Multi (3)	Unknown	White and Klitgord, 1976; Kopp et al., 2000; Bourget et al., 2011
Definitions											i.e. coarse (sand)/ fine(clays)	Rea et al., 1996		Kottek et al., 2006										

(orange) channel terminates in trench
(yellow) channel escapes trench

References

Ballance, P.F., Scholl, D.W., Vallier, T.L., Stevenson, A.J., Ryan, H. and Herzer, R.H., 1989. Subduction of a Late Cretaceous seamount of the Louisville Ridge at the Tonga Trench: A model of normal and accelerated tectonic erosion. *Tectonics*, *8* (5), pp.953-962.
Bourget, J., Zaragosi, S., Ellouz-Zimmermann, N., Mouchot, N., Garlan, T., SCHNEIDER, J.L., Lanfumey, V. and Lallemant, S., 2011. Turbidite system architecture and sedimentary processes along topographically complex slopes: the Makran convergent margin. *Sedimentology*, *58* (2), pp.376-406.
Brun, J.P. and Sokoutis, D., 2010. 45 my of Aegean crust and mantle flow driven by trench retreat. *Geology*, *38* (9), pp.815-818.
Callec, Y., Deville, E., Desaubliaux, G., Griboulard, R., Huyghe, P., Mascle, A., Mascle, G., Noble, M., Padron de Carillo, C. and Schmitz, J., 2010. The Orinoco turbidite system: Tectonic controls on sea-floor morphology and sedimentation. *AAPG bulletin*, *94* (6), pp.869-887.
Clift, P.D., MacLeod, C.J., Tappin, D.R., Wright, D.J. and Bloomer, S.H., 1998. Tectonic controls on sedimentation and diagenesis in the Tonga Trench and forearc, southwest Pacific. *Geological Society of America Bulletin*, *110* (4), pp.483-496.
Collot, J.Y., Lamarche, G., Wood, R.A., Delteil, J., Sosson, M., Lebrun, J.F. and Coffin, M.F., 1995. Morphostructure of an incipient subduction zone along a transform plate boundary: Puysegur Ridge and Trench. *Geology*, *23* (6), pp.519-522.
Collot, J.Y., Charvis, P., Gutscher, M.A. and Operto, S., 2002. Exploring the Ecuador -Colombia active margin and interplate seismogenic zone. *EOS, Transactions American Geophysical Union*, *83* (17), pp.185-190.
Curray, J.R., Emmel, F.J. and Moore, D.G., 2002. The Bengal Fan: morphology, geometry, stratigraphy, history and processes. *Marine and Petroleum Geology*, *19* (10), pp.1191-1223.
Davis, E.E. and Hyndman, R.D., 1989. Accretion and recent deformation of sediments along the northern Cascadia subduction zone. *Geological Society of America Bulletin*, *101* (11), pp.1465-1480.
Davies, H.L., Keene, J.B., Hashimoto, K., Joshima, M., Stuart, J.E. and Tiffin, D.L., 1986. Bathymetry and canyons of the western Solomon Sea. *Geo-Marine Letters*, *6* (4), pp.181-191
Delong, S.E., Fox, P.J. and McDowell, F.W., 1978. Subduction of the Kula ridge at the Aleutian trench. *Geological Society of America Bulletin*, *89* (1), pp.83-95.
Deville, E., Mascle, A., Callec, Y., Huyghe, P., Lallemant, S., Lerat, O., Mathieu, X., De Carillo, C.P., Patriat, M., Pichot, T. and Loubrieux, B., 2015. Tectonics and sedimentation interactions in the east Caribbean subduction zone: an overview from the Orinoco delta and the Barbados accretionary prism. *Marine and Petroleum Geology*, *64*, pp.76-103.
Exon, N.F. and Tiffin, D.L., 1982. Geology and petroleum prospects of offshore New Ireland Basin in northern Papua New Guinea.
Fisher, M.A., Collot, J.Y. and Geist, E.L., 1991. Structure of the collision zone between Bougainville Guyot and the accretionary wedge of the New Hebrides island arc, Southwest Pacific. *Tectonics*, *10* (5), pp.887-903.
Fryer, P., 1995. Geology of the Mariana trough. In *Backarc Basins* (pp. 237-279). Springer, Boston, MA.
Gavey, R., Carter, L., Liu, J.T., Talling, P.J., Hsu, R., Pope, E. and Evans, G., 2017. Frequent sediment density flows during 2006 to 2015, triggered by competing seismic and weather events: Observations from subsea cable breaks off southern Taiwan. *Marine Geology*, *384*, pp.147-158.
Gnibidenko, H., Bykova, T.G., Veselov, O.V., Vorobiev, V.M. and Svarichevsky, A.S., 1983. The Tectonics of the Kuril -Kamchatka Deep -Sea Trench. *Geodynamics of the Western Pacific -Indonesian Region*, *11*, pp.249-285.
Goldfinger, C., Nelson, C.H., Morey, A.E., Johnson, J.E., Patton, J.R., Karabanov, E.B., Gutierrez-Pastor, J., Eriksson, A.T., Gràcia, E., Dunhill, G. and Enkin, R.J., 2012. *Turbidite event history--Methods and implications for Holocene paleoseismicity of the Cascadia subduction zone* (No. 1661-F). US Geological Survey.
Hayes, D.E. and Lewis, S.D., 1984. A geophysical study of the Manila Trench, Luzon, Philippines: 1. Crustal structure, gravity, and regional tectonic evolution. *Journal of Geophysical Research: Solid Earth*, *89* (B11), pp.9171-9195.
Huchon, P., Lybéris, N., Angelier, J., Le Pichon, X. and Renard, V., 1982. Tectonics of the Hellenic Trench: a synthesis of Sea-Beam and submersible observations. *Tectonophysics*, *86* (1-3), pp.69-112.
Huh, C.A., Lin, H.L., Lin, S. and Huang, Y.W., 2009. Modern accumulation rates and a budget of sediment off the Gaoping (Kaoping) River, SW Taiwan: a tidal and flood dominated depositional environment around a submarine canyon. *Journal of Marine Systems*, *76* (4), pp.405-416.
Kulm, L.D., 1981. Peru continental margin and trench. *Nazca Plate: Crustal Formation and Andean Convergence: a Volume Dedicated to George P. Woollard*, *154*, p.445.
Komar, P.D., 1973. Continuity of turbidity current flow and systematic variations in deep-sea channel morphology. *Geological Society of America Bulletin*, *84* (10), pp.3329-3338.
Kopp, C., Fruehn, J., Flueh, E.R., Reichert, C., Kukowski, N., Bialas, J. and Klaeschen, D., 2000. Structure of the Makran subduction zone from wide-angle and reflection seismic data. *Tectonophysics*, *329* (1-4), pp.171-191.
Kottek, M., Grieser, J., Beck, C., Rudolf, B. and Rubel, F., 2006. World map of the Köppen-Geiger climate classification updated. *Meteorologische Zeitschrift*, *15* (3), pp.259-263.
Krabbenhöft, A., Bialas, J., Kopp, H., Kukowski, N. and Hübscher, C., 2004. Crustal structure of the Peruvian continental margin from wide-angle seismic studies. *Geophysical Journal International*, *159* (2), pp.749-764.
Lallemand, S.E., Popoff, M., Cadet, J.P., Bader, A.G., Pubellier, M., Rangin, C. and Deffontaines, B., 1998. Genetic relations between the central and southern Philippine Trench and the Sangihe Trench. *Journal of Geophysical Research: Solid Earth*, *103* (B1), pp.933-950.
Larter, R.D., Vanneste, L.E., Morris, P. and Smythe, D.K., 2003. Structure and tectonic evolution of the South Sandwich arc. *Geological Society, London, Special Publications*, *219* (1), pp.255-284.
Larue, D.K. and Ryan, H.F., 1998. Seismic reflection profiles of the Puerto Rico Trench: Shortening between the North American and Caribbean plates. *SPECIAL PAPERS-GEOLOGICAL SOCIETY OF AMERICA*, pp.193-210.
Lewis, K.B., 1994. The 1500-km-long Hikurangi Channel: trench-axis channel that escapes its trench, crosses a plateau, and feeds a fan drift. *Geo-Marine Letters*, *14* (1), pp.19-28.
Lewis, S.D. and Hayes, D.E., 1984. A geophysical study of the Manila Trench, Luzon, Philippines: 2. Fore arc basin structural and stratigraphic evolution. *Journal of Geophysical Research: Solid Earth*, *89* (B11), pp.9196-9214.
López, A.M., Stein, S., Dixon, T., Sella, G., Calais, E., Jansma, P., Weber, J. and LaFemina, P., 2006. Is there a northern Lesser Antilles forearc block?. *Geophysical research letters*, *33* (7).
Mann, P. and Taira, A., 2004. Global tectonic significance of the Solomon Islands and Ontong Java Plateau convergent zone. *Tectonophysics*, *389* (3-4), pp.137-190.
McMillen, K.J., Enkeboll, R.H., Moore, J.C., Shipley, T.H. and Ladd, J.W., 1982. Sedimentation in different tectonic environments of the Middle America Trench, southern Mexico and Guatemala. *Geological Society, London, Special Publications*, *10* (1), pp.107-119.
Meckel, T.A., Coffin, M.F., Mosher, S., Symonds, P., Bernardel, G. and Mann, P., 2003. Underthrusting at the Hjort Trench, Australian -Pacific plate boundary: Incipient subduction?. *Geochemistry, Geophysics, Geosystems*, *4* (12).
Melhuish, A., Sutherland, R., Davey, F.J. and Lamarche, G., 1999. Crustal structure and neotectonics of the Puysegur oblique subduction zone, New Zealand. *Tectonophysics*, *313* (4), pp.335-362.
Minelli, L. and Faccenna, C., 2010. Evolution of the Calabrian accretionary wedge (central Mediterranean). *Tectonics*, *29* (4).
Milsom, J., Masson, D., Nichols, G., Sikumbang, N., Dwiyanto, B., Parson, L. and Kallagher, H., 1992. The Manokwari trough and the western end of the New Guinea trench. *Tectonics*, *11* (1), pp.145-153.
Moore, G.F., Curray, J.R. and Emmel, F.J., 1982a. Sedimentation in the Sunda Trench and forearc region. *Geological Society, London, Special Publications*, *10* (1), pp.245-258.
Moore, J.C., Watkins, J.S., McMillen, K.J., Bachman, S.B., Leggett, J.K., Lundberg, N., Shipley, T.H., Stephan, J.F., Beghtel, F.W., Butt, A. and Didyk, B.M., 1982b. Facies belts of the Middle America Trench and forearc region, southern Mexico: results from Leg 66 DSDP. *Geological Society, London, Special Publications*, *10* (1), pp.77-94.
Mosher, D.C., Austin Jr, J.A., Fisher, D. and Gulick, S.P.S., 2008. Deformation of the northern Sumatra accretionary prism from high-resolution seismic reflection profiles and ROV observations. *Marine Geology*, *252* (3-4), pp.89-99.
Mountney, N.P. and Westbrook, G.K., 1997. Quantitative analysis of Miocene to Recent forearc basin evolution along the Colombian convergent margin. *Basin Research*, *9* (3), pp.177-196.
Mountjoy, J.J., Howarth, J.D., Orpin, A.R., Barnes, P.M., Bowden, D.A., Rowden, A.A., Schimel, A.C., Holden, C., Horgan, H.J., Nodder, S.D. and Patton, J.R., 2018. Earthquakes drive large-scale submarine canyon development and sediment supply to deep-ocean basins. *Science advances*, *4* (3), p.eaar3748.
Ness, G.E. and Kulm, L.D., 1973. Origin and development of Surveyor deep-sea channel. *Geological Society of America Bulletin*, *84* (10), pp.3339-3354.
Nichols, G., Hall, R., Milsom, J., Masson, D., Parson, L., Sikumbang, N., Dwiyanto, B. and Kallagher, H., 1990. The southern termination of the Philippine Trench. *Tectonophysics*, *183* (1-4), pp.289-303.
Nishizawa, A., Kaneda, K., Oikawa, M., Horiuchi, D., Fujioka, Y. and Okada, C., 2017. Variations in seismic velocity distribution along the Ryukyu (Nansei-Shoto) Trench subduction zone at the northwestern end of the Philippine Sea plate. *Earth, Planets and Space*, *69* (1), p.86.
Phinney, E.J., Mann, P., Coffin, M.F. and Shipley, T.H., 2004. Sequence stratigraphy, structural style, and age of deformation of the Malaita accretionary prism (Solomon arc–Ontong Java Plateau convergent zone). *Tectonophysics*, *389* (3-4), pp.221-246.
Pickering, K.T., Pouderoux, H., McNeill, L.C., Backman, J., Chemale, F., Kutterolf, S., Milliken, K.L., Hideki, M., Henstock, T.J., Stevens, D.E. and Parnell, C., 2020. Sedimentology, stratigraphy and architecture of the Nicobar Fan (Bengal–Nicobar Fan System), Indian Ocean: Results from International Ocean Discovery Program Expedition 362. *Sedimentology*.
Polonia, A., Torelli, L., Mussoni, P., Gasperini, L., Artoni, A. and Klaeschen, D., 2011. The Calabrian Arc subduction complex in the Ionian Sea: Regional architecture, active deformation, and seismic hazard. *Tectonics*, *30* (5).
Rea, D.K. and Ruff, L.J., 1996. Composition and mass flux of sediment entering the world's subduction zones: implications for global sediment budgets, great earthquakes, and volcanism. *Earth and Planetary Science Letters*, *140* (1-4), pp.1-12.
Scholl, D.W., 1974. Sedimentary sequences in the north Pacific trenches. In *The geology of continental margins* (pp. 493-504). Springer, Berlin, Heidelberg.
Schweller, W.J. and Kulm, L.D., 1978. Extensional rupture of oceanic crust in the Chile Trench. *Marine Geology*, *28* (3-4), pp.271-291.
Shimamura, K., 1989. Topography and sedimentary facies of the Nankai deep sea channel. *Sedimentary Facies in the Active Plate Margin. Terrapub, Tokyo*, *529*, p.556.
Soh, W., Taira, A. and Tokuyama, H., 1988. A trench fan in the Izu-Ogasawara Trench on the Boso Trench triple junction, Japan. *Marine geology*, *82* (3-4), pp.235-249.
Stanley, D.J. and Maldonado, A., 1981. Depositional models for fine -grained sediment in the western Hellenic Trench, Eastern Mediterranean. *Sedimentology*, *28* (2), pp.273-290.
Stern, R.J. and Bloomer, S.H., 1992. Subduction zone infancy: examples from the Eocene Izu-Bonin-Mariana and Jurassic California arcs. *Geological Society of America Bulletin*, *104* (12), pp.1621-1636.
Taira, A., Mann, P. and Rahardiawan, R., 2004. Incipient subduction of the Ontong Java Plateau along the North Solomon trench. *Tectonophysics*, *389* (3-4), pp.247-266.
Thornburg, T.M., Kulm, L.D. and Hussong, D.M., 1990. Submarine-fan development in the southern Chile Trench: a dynamic interplay of tectonics and sedimentation. *Geological Society of America Bulletin*, *102* (12), pp.1658-1680.
Tiffin, D.L., Davies, H.L., Honza, E., Lock, J. and Okuda, Y., 1987. The New Britain Trench and 149 Embayment, western Solomon Sea. *Geo-marine letters*, *7* (3), pp.135-142.
Tregoning, P., Lambeck, K., Stolz, A., Morgan, P., McClusky, S.C., van der Beek, P., McQueen, H., Jackson, R.J., Little, R.P., Laing, A. and Murphy, B., 1998a. Estimation of current plate motions in Papua New Guinea from Global Positioning System observations. *Journal of Geophysical Research: Solid Earth*, *103* (B6), pp.12181-12203.
Tregoning, P., Tan, F., Gilliland, J., McQueen, H. and Lambeck, K., 1998b. Present -day crustal motion in the Solomon Islands from GPS observations. *Geophysical research letters*, *25* (19), pp.3627-3630.
Tregoning, P. and Gorbatov, A., 2004. Evidence for active subduction at the New Guinea Trench. *Geophysical Research Letters*, *31* (13).
Underwood, M.B., 1986. Transverse infilling of the central Aleutian Trench by unconfined turbidity currents. *Geo-Marine Letters*, *6* (1), pp.7-13.
Underwood, M.B., Saito, S. and Kubo, Y., the Expedition 322 Scientists, 2010. Expedition 322 summary. *Saito, S., Underwood, MB, Kubo, Y., and the Expedition*, *322*.
Uchupi, E. and Emery, K.O., 1963, October. The continental slope between San Francisco, California and Cedros Island, Mexico. In *Deep Sea Research and Oceanographic Abstracts* (Vol. 10, No. 4, pp. 397-447). Elsevier.
von Huene, R., Langseth, M., Nasu, N. and Okada, H., 1982. A summary of Cenozoic tectonic history along the IPOD Japan Trench transect. *Geological Society of America Bulletin*, *93* (9), pp.829-846.
Watkins, J.S., 1989. The Middle America trench off southern Mexico. *The Eastern Pacific Ocean and Hawaii, The Geology of North America*, pp.523-533.
Westbrook, G.K., Mascle, A. and Biju-Duval, B., 1984. Geophysics and the structure of the Lesser Antilles Forearc. *Initial Reports of the Deep Sea Drilling Project*, *78*, pp.23-38.
White, R.S. and Klitgord, K., 1976. Sediment deformation and plate tectonics in the Gulf of Oman. *Earth and Planetary Science Letters*, *32* (2), pp.199-209.
Wolf, S.C. and Hamer, M.R., 1999. *Turbidite pathways in Cascadia Basin and Tufts abyssal plain, Part A, Astoria Channel, Blanco Valley, and Gorda Basin* (No. 99-157). US Geological Survey.
Zellmer, K.E. and Taylor, B., 2001. A three -plate kinematic model for Lau Basin opening. *Geochemistry, Geophysics, Geosystems*, *2* (5).

Supplementary material 2. Statistical methodology

Data were collected from published sources (see Supplement 1) and when not available in the literature, measurements were made using GeomapApp© (Ryan et al., 2009), which offers a range of bathymetry datasets in trenches, all of which provide sufficient resolution to conduct our analysis. Hence, the metadata study was not significantly limited by data quality or availability in forearc subduction trenches.

Multivariate statistical analysis of the subduction trenches dataset (see Supplement 5) was conducted using Python *numpy* and *pandas* software (Mckinney, 2011). Principle components analysis (PCA) determines theoretical, dimensionless variables (components) that account for as much variance as possible in the dataset, in order to display linear variations and identify the most important variables in the dataset (Wold et al., 1987). The two most important variables, or components, with the largest influence on the dataset can then be plotted for visual analysis of sample distribution and grouping. Other forms of analysis, such as Correspondence Analysis were conducted, with PCA found to respond best to the dataset.

Before entering the data to the software variables with a large range (e.g. trench width and convergence rate) were averaged to their mean and the dataset was standardized to comparable scales. The percentage and eigenvalue of each variable is listed below (Table S2). Sensitivity analysis was conducted by running the dataset solely for trenches with an axial channel; for those without channels; and on a dataset without the channel information (Fig S4); no significant deviation from the observed trends was encountered. Further investigations, removing selected low value and high value variables from the analysis, including those identified as the key variables (trench length, sediment cover or sediment supply) did not demonstrate groupings of trenches with and without channels (Fig. S5), giving confidence in interpretation of the key variables.

PCA interpretation is based on the production of biplots, which indicate the governing variable on each component and hence each axis of the plots, and empirical observations of where the data points plot in relation to the components. Trench length shows the greatest affinity with component 1 (43% of variance); component 2 is associated with thickness of sedimentary cover (36% of variance); and component 3 is related to sediment supply (20% of variance). No other component accounted for >1% of variance (Table S2). The results are displayed as a scatter plot of the two variables that demonstrated the most variance.

Table S2. Principle components (PC) scores.

PC	1	2	3	4	5	6	7	8	9	10	11	12
Eigenvalue	1.92E+06	1.61E+06	874832	26626.7	4905.65	1621.58	887.901	451.656	293.249	49.9579	23.1808	21.8994
% variance	43.232	36.276	19.706	0.59978	0.1105	0.036527	0.02	0.010174	0.006606	0.001125	0.000522	0.000493

PC	13	14	15	16	17	18	19	20	21	22	23	24
Eigenvalue	13.0941	2.41232	1.34224	0.748273	0.404888	0.206116	0.141873	0.125699	0.08908	0.042666	0.018016	0.001184
% variance	0.000295	5.43E-05	3.02E-05	1.69E-05	9.12E-06	4.64E-06	3.20E-06	2.83E-06	2.01E-06	9.61E-07	4.06E-07	2.67E-08

References

McKinney, W., 2011, pandas: a foundational Python library for data analysis and statistics: Python for High Performance and Scientific Computing, v. 14, p.1-9.

Ryan, W. B. F., Carbotte, S.M., Coplan, J., O'Hara, S., Melkonian, A., Arko, R., Weissel, R.A., Ferrini, V., Goodwillie, A., Nitsche, F., Bonczkowski, J., and Zemsky, R., 2009, Global Multi-Resolution Topography (GMRT) synthesis data set: Geochemistry, Geophysics, Geosystems, v. 10, Q03014.

Wold, S., Esbensen, K. and Geladi, P., 1987, Principal component analysis: Chemometrics and intelligent laboratory systems, v. 2, p.37-52.

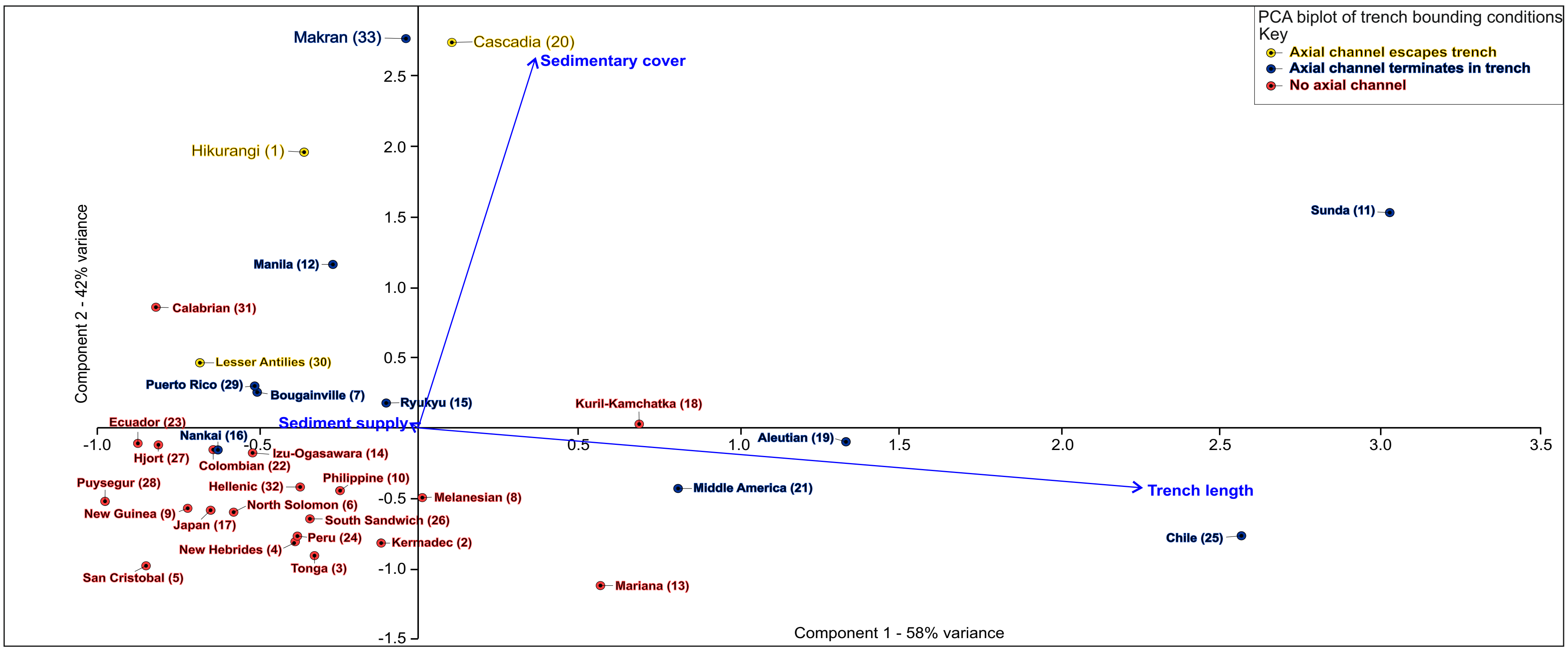

Fig. S4. Principle components analysis biplot (eigenvalue scale) of trench geomorphological factors considering only trench variables (not channels).

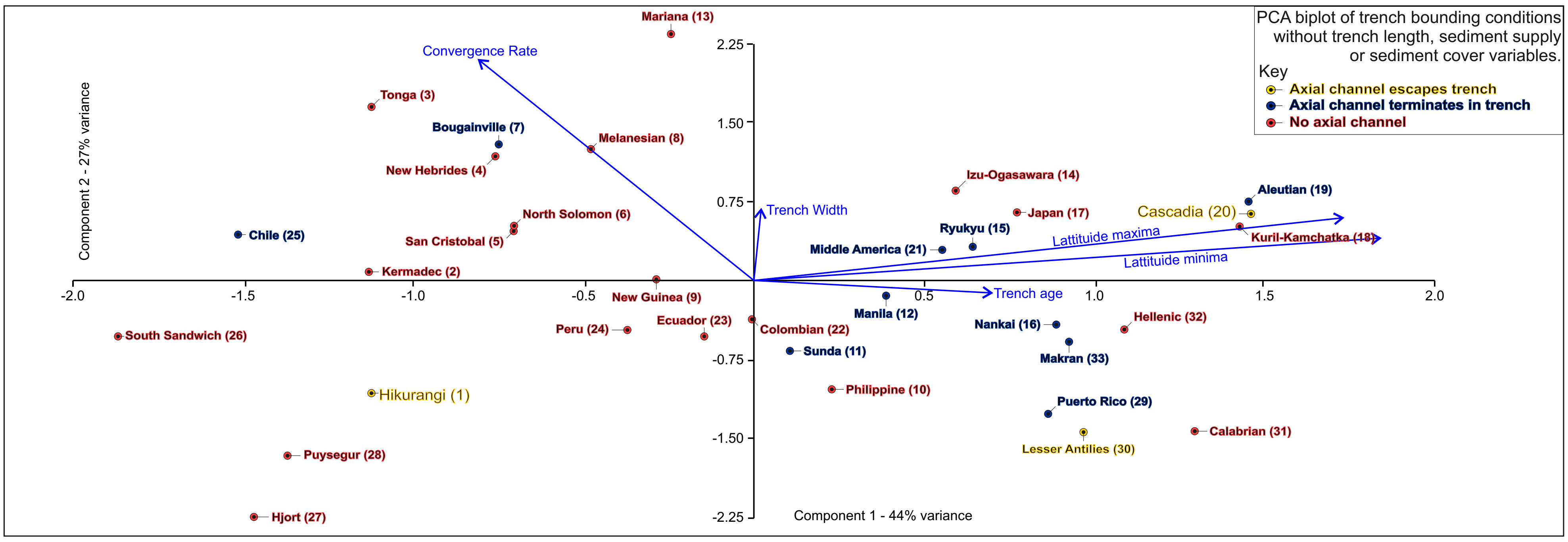

Fig. S5. Principle components analysis biplot (eigenvalue scale) of trench geomorphological factors considering only trench variables, without trench length, sediment cover or sediment supply; without variables identified as the key controls, trenches with or without channels show no relation.